

Don't Count on One to Carry the Ball

Scaling BFT without Sacrificing Efficiency

Kexin Hu
Institute of Software, Chinese
Academy of Sciences
hukexin@iscas.ac.cn

Kaiwen Guo
University of Chinese Academy of
Sciences
kaiwen2016@iscas.ac.cn

Qiang Tang
The University of Sydney
qiang.tang@sydney.edu.au

Zhenfeng Zhang
Institute of Software, Chinese
Academy of Sciences
zhenfeng@iscas.ac.cn

Hao Cheng
University of Chinese Academy of
Sciences
chenghao2020@iscas.ac.cn

Zhiyang Zhao
University of Chinese Academy of
Sciences
zhiyang2018@iscas.ac.cn

ABSTRACT

As the emergence of large-scale decentralized applications, a scalable and efficient Byzantine Fault Tolerant (BFT) protocol of hundreds of replicas is ideal. Although the throughput of existing leader-based BFT protocols has reached a high level of 10^5 operations per second for a small scale of replicas, it drops significantly when the number of replicas increases, which leads to a lack of practicality.

This paper focuses on the scalability of BFT protocols and identifies a major bottleneck to leader-based BFT protocols due to the excessive workload of the leader at large scales. A new metric of *scaling factor* is defined to capture whether a BFT protocol will get stuck when it scales out, which can be used to measure the performance of efficiency and scalability of BFT protocols. We propose “Leopard”, the first leader-based BFT protocol that scales to multiple hundreds of replicas, and more importantly, preserves a high efficiency. It is secure with the optimal resilience bound (i.e., $1/3$) in the partial synchronous network model. We remove the bottleneck by introducing a technique of achieving *constant* scaling factor, which takes full advantage of the idle resource and adaptively balances the workload of the leader among all replicas. The proposed Leopard protocol also allows a parallel execution for different agreement instances and each is achieved via two rounds of voting with a linear communication complexity.

We implement Leopard and evaluate its performance compared to HotStuff, the state-of-the-art BFT protocol. We run extensive experiments on the two systems back-to-back in the same environments with up to 600 replicas. The results show that Leopard achieves significant performance improvements both on throughput and scalability. In particular, the throughput of Leopard remains at a high level of 10^5 when the system scales out to 600 replicas. It achieves a $5\times$ throughput over HotStuff when the scale is 300 (which is already the largest scale we can see the progress of the latter in our experiments), and the gap becomes wider as the number of replicas further increases.

KEYWORDS

Byzantine fault tolerance; scalability; high-efficiency; partial synchronous model; optimal resilience bound;

1 INTRODUCTION

Byzantine fault tolerance (BFT) protocols aim to enable a set of replicas to reach consensus, and endure arbitrary failures from a subset of these replicas. A BFT protocol guarantees *safety* that honest replicas’ outputs are consistent, and *liveness* that honest inputs will be output by every other honest replica. As a fundamental primitive in distributed computing, it has been studied for decades in many classical works, e.g., [43, 54, 56], and received revived attention showing substantial improvements, e.g., [13, 15, 31, 64].

Traditional BFT solutions [2, 17, 32] that ensure safety and liveness without relaxing the $1/3$ resilience bound normally support for a small scale of replicas (e.g., a dozen replicas) with a moderate throughput (e.g., a few thousand operations per second), mostly due to their heavy communication costs. Great efforts have been made on the way to reduce the cost. Recent interesting ideas [31, 64] have brought it down from quadratic communication to linear. Evaluations show that they achieve a high throughput of 10^5 operations per second [65].

Since the emergence of decentralized applications on the Internet started from Bitcoin [49], even consortium blockchain may have a large number of peers (e.g., in a global supply-chain); moreover, BFT protocols are often adopted as an important component for the permissionless consensus (e.g., [27, 40, 46]) and proof-of-stake protocols (e.g., Algorand [30]), in which a large number of committee members (thousands) are chosen to run a BFT protocol. It follows that BFT protocols that can support a large number of replicas have become highly demanded.

A practical BFT protocol should thus perform well on efficiency and scalability simultaneously, i.e., preserving a high throughput when the number of replicas increases¹.

Unfortunately, the latest evaluation results (Fig.1) of the state-of-the-art BFT proposals, HotStuff [64] and BFT-SMaRt [9], with at most 128 replicas show that, the high throughput is only achieved on a small scale of replicas; when the number of replicas increases, the throughput drops sharply! It follows that all those BFT protocols still face a scalability-efficiency dilemma.

Two common methods in distributed systems to improve scalability and efficiency are scaling out (or horizontal scaling) and scaling

¹Algorand [30] provides a “scalable” BFT solution that supports thousands of nodes. However, the throughput is only about 1000, while we would like to have both scalability and the high efficiency.

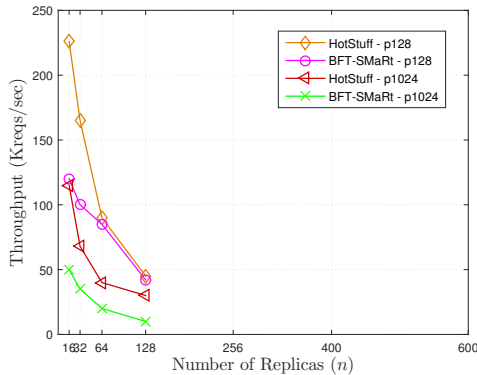


Figure 1: Evaluation result [65] on the measure of throughput with different scales of replicas in HotStuff [64] and BFT-SMaRt [9], under 128-byte and 1024-byte payload sizes.

up (or vertical scaling). Scaling out is to add more replicas and different replicas deal with distinct pending requests, thus it increases the total process capacity. The popular method for scaling out in the Byzantine fault tolerant setting is via sharding [40, 46, 67]. The set of replicas are divided into disjoint subsets (or shards), where each subset usually runs a BFT protocol to process requests in parallel with other subsets. However, the basis of a valid sharding solution is a BFT protocol supporting multiple hundreds of replicas and providing high efficiency. This is due to that, the size of each subset should be big enough to ensure the 1/3 resilience bound is satisfied to guarantee a secure confirmation. It can be seen (in §2) that multiple hundreds of replicas are necessary. Scaling up is to add more resources to each replica. An effective scaling up should significantly increase the performance of the protocol by adding a reasonable of resources. However, we find out (shown in §6) that when the number of replicas is large, the increased throughput in the current leader-based BFT protocol approaches 0 by configuring with more bandwidths. This observation motivates us to consider the following question:

Can we design a scalable BFT protocol that can support multiple hundreds of replicas, and more importantly, preserve the high-efficiency and enable an effective scaling up?

1.1 Our Contributions

A consensus protocol usually contains two basic steps: *data delivery* and *agreement*, where the former is to synchronize data (i.e., pending requests) among all replicas, and the latter is to reach an agreement on the synchronized data which is often achieved by several rounds of voting among replicas in a BFT protocol. Most of the efficient BFT protocols (such as HotStuff) are leader-based constructions where a leader replica generates a consensus proposal (e.g., the new block) containing a bunch of pending requests, and distributes it to all the other replicas. This works for completing the data delivery as well as indicating the start of the agreement on the delivered consensus proposal. In this paper, we focus on scalable and efficient leader-based (partially synchronous) BFT protocols. Our contributions are three-fold:

Identifying the major bottleneck. Let us first review the evolution to the state-of-the-art solution, then examine the major reason of the sharp efficiency drop in existing BFT protocols (shown in Fig. 1).

The traditional leader-based BFT (such as the seminal PBFT [17]) suffers from the expensive quadratic communication cost mostly due to its all-to-all voting pattern during the agreement. Tremendous progress [7, 20, 32, 41, 44] has been achieved towards conquering this challenge. In particular, one can reduce the quadratic message complexity to linear by using a collector [41] to collect votes from replicas and then disseminate the collected vote set to everyone. When further combined with the threshold signature schemes [12, 59] such that each vote from a replica is instantiated by a threshold signature share, the size of the vote set which contains only one aggregated threshold signature is reduced from linear to even constant, thus reducing the protocol to a linear vote-complexity² [31, 64]. Besides, a conventional optimization was running the consensus on the digest of consensus proposals to further reduce the communication cost.

A more intriguing question emerges: despite those major improvements, why do the state-of-the-art leader-based BFT protocols still suffer from the scalability-efficiency dilemma (its throughput drops sharply as n increases, see Fig. 1)?

While those protocols mainly focus on reducing the cost of the protocol overall measured by the total number of votes, one crucial but often neglected aspect in a leader-based BFT protocol is that the *leader* might be overloaded. To validate this in practice, we conducted an experimental evaluation of the leader’s workload in a leader-based BFT protocol with an increasing n . We use the leader’s bandwidth utilization to indicate its workload since the bandwidth’s consumption can be easily measured. We chose HotStuff [64] as a typical example of the state-of-the-art leader-based BFT protocol. Fig. 2 presents the evaluation result with a fixed 128-byte payload size. It shows that the leader’s bandwidth utilization increases significantly as the protocol scale getting larger.

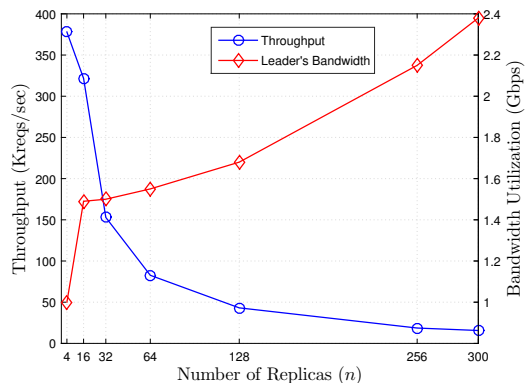


Figure 2: Throughput and leader’s bandwidth utilization of HotStuff using implementation from [66].

²Similar to the authenticator-complexity defined in HotStuff [64], this complexity measure indicates the sum, over all replicas, of the number of votes/authenticators received by each replica in the protocol to reach a consensus decision in the optimistic case.

Recall that, the leader serves as disseminating pending requests to all the other $n - 1$ replicas in most leader-based BFT protocols. Let n be the number of replicas, Λ denote the total bits of requests processed per second by the protocol³. The workload of the leader on disseminating the pending requests per second can be expressed as

$$\Gamma_{\text{leader}}^{\text{pre-send}} = \Lambda \times (n - 1), \quad (1)$$

which is proportional to n by a factor of Λ . Since we want to achieve the high efficiency, Λ must be a large value. Hence, the leader’s workload is prohibitively high on a large scale. This makes that the protocol cannot perform well on efficiency and scalability simultaneously. Even worse, due to the bottleneck effect of the leader, it’s hard to effectively improve the protocol’s performance by adding resources at each replica when the scale of the protocol is large.

To preserve high efficiency for a BFT protocol when the protocol’s scale increases, the heaviest workload among replicas should not be a bottleneck when n increases. To capture this, we define a performance metric called *scaling factor* to be the heaviest workload on processing per bit of requests among replicas per second, i.e.,

$$SF = \max_{1 \leq i \leq n} \{\Gamma_i\} / \Lambda$$

where Γ_i is the workload on processing pending requests at replica i per second.

Let’s take HotStuff as an example to evaluate the scaling factor (SF) Let $\Gamma_{\text{non-leader}}^{\text{pre-recv}}$ denote the workload on processing all requests received from the leader for each non-leader replica, and we have that

$$\begin{aligned} SF^{\text{pre}} &= \max\{\Gamma_{\text{leader}}^{\text{pre-send}}, \Gamma_{\text{non-leader}}^{\text{pre-recv}}\} / \Lambda \\ &= \max\{\Lambda \times (n - 1), \Lambda\} / \Lambda \\ &= (n - 1), \end{aligned}$$

which grows linearly with respect to the number of replicas n .

Usually, SF is a non-decreasing function of n for leader-based BFT protocols. If per replica’s processing capacity is bounded by Γ , then the protocol’s throughput is less than Γ / SF , which will decrease with the growth of n . To make the throughput be well preserved when the protocol’s scale increases, it would be desirable to design a protocol that has a scaling factor that grows slower, and in the ideal case, just a constant, and irrelevant to n !

Besides, the effectiveness of the performance’s improvement by adding resources, i.e., scaling up the system, can be expressed as the ratio of the increased bits Λ^Δ of requests processed per second by the protocol over the heaviest increasable workload W^Δ on processing pending requests per second among replicas. This indicates the cost-effectiveness of the protocol, and we have

$$\begin{aligned} \left(\frac{\Lambda^\Delta}{W^\Delta}\right)^{\text{pre}} &= \Lambda^\Delta / \max_{1 \leq i \leq n} \{\Gamma_i^\Delta\} \\ &= \Lambda^\Delta / (\Gamma_{\text{leader}}^\Delta)^{\text{pre-send}} \\ &= \frac{1}{n - 1}, \end{aligned} \quad (2)$$

which decreases linearly with respect to n . It means that, the increase of throughput approaches to 0 when $n \rightarrow +\infty$.

³Compared to the throughput, a performance metric of the protocol that passively measured by the experimental evaluation, Λ captures the processing capacity of the protocol which is an inherent property of the protocol.

A scalable and efficient BFT. We present “Leopard”, a scalable and efficient BFT protocol in the partial synchronous network model. Leopard preserves the high efficiency while scaling out, thus it provides the first solution to the scalability-efficiency dilemma of existing leader-based BFT protocols. The protocol achieves a desirable scaling factor that is irrelevant to the scale of the protocol. Meanwhile, the agreement of consensus proposals in our protocol is parallel-executed with a linear communication complexity, and our protocol features the hallmark of *optimistic responsiveness* [52]. The safety of the protocol can be guaranteed even in the asynchronous network assumption where there is no time bound on message delivery, while the liveness relies on the synchronous assumption as most BFT protocols of the same kind [17–19, 31, 58, 64]. Let us briefly walk through the ideas.

Balancing the workload. Most leader-based BFT protocols, relying on the leader to disseminate pending requests to all replicas, incur high communication overhead at the leader. Therefore, the leader becomes the “Achilles heel” of these protocols when they scale out.

To resolve this, our protocol amortizes the leader’s workload by taking full advantage of the idle resource of other replicas. We decouple a BFT consensus proposal into two planes: *Pending requests* and *indicators each to a package of pending requests*. Every non-leader replica packs the pending requests in its buffer and disseminates the package to all the others, whereby the leader only has to include an indicator to each outstanding package in a consensus proposal.

Let α be the number of bits in a package and β denote the size of an indicator, the scaling factor of Leopard will be

$$\begin{aligned} SF^{\text{ours}} &= \max\{\Gamma_{\text{leader}}^{\text{ours-send}} + \Gamma_{\text{leader}}^{\text{ours-recv}}, \Gamma_{\text{non-leader}}^{\text{ours-send}} + \Gamma_{\text{non-leader}}^{\text{ours-recv}}\} / \Lambda \\ &\approx \max\{\Lambda \times \frac{\beta}{\alpha} \times (n - 1) + \Lambda, 2 \cdot \Lambda + \Lambda \times \frac{\beta}{\alpha}\} / \Lambda \\ &= \max\{\frac{\beta(n - 1)}{\alpha} + 1, 2 + \frac{\beta}{\alpha}\}. \end{aligned}$$

Note that, $\alpha \geq 1$ is a parameter. When the scale of the protocol increases, we can adaptively adjust α with a larger value in order to counteract the effect by an increasing n . In this way, the scaling factor of our protocol remains constant as n increases.

Ideally, the ratio of Λ^Δ over W^Δ is 1. Instead of a value approaching 0 as in most previous protocols (see Eq. (2)), Leopard achieves better cost-effectiveness with a constant ratio of about 1/2 for all scales of the protocol. Hence, Leopard removes the major bottleneck and provides a better solution to the two problems simultaneously.

Further improving the protocol design. Having the main advantage as stated above, we still need to make the remaining part of the protocol friendly to support multiple hundreds of replicas.

Reaching an agreement on pending requests is achieved by the normal-case mode of a BFT protocol, and this happens most of the time. Agreement instances in Leopard are concurrently executed and each instance consists of a two-round of voting. Besides, Leopard has the desirable optimistic responsiveness, that in the optimistic case of an honest leader, our protocol proceeds as network delivers. This further helps Leopard to be a highly efficient BFT solution.

Also, leveraging known techniques [31, 64], we reduce the communication complexity of the protocol overall by one order of n ,

using the threshold signature scheme and involving a collector to do the aggregation of threshold signature shares. Hence, each vote during the agreement is instantiated by a threshold signature share, while the proof for the completion of a round of voting is thus an aggregated threshold signature that combines enough votes (or threshold signature shares). This results in a protocol with a linear communication complexity for the agreement during the normal-case mode, and a quadratic communication complexity for replacing a Byzantine leader during the view-change mode.

Implementation and experimental evaluations. We design and implement a prototype BFT system based on Leopard. We evaluate its performance with up to 600 replicas. For a fair comparison, we deploy both Leopard and HotStuff back-to-back in the same environment of (c5.xlarge) Amazon EC2 instances. Since current HotStuff implementation by its authors [65] can hardly work when $n > 300$, we only compare the results of HotStuff with n up to 300.

Fig. 3 presents the main result of this paper with a Byzantine replica number to the largest possible one (i.e., touching the $1/3$ optimal resilience bound). It shows that, the throughput of Leopard remains almost flat and achieves around 10^5 for replica number varies up to 600. Compared to HotStuff, Leopard achieves $5\times$ throughput when n scales to 300. It shows that the gap becomes wider with an even larger protocol scale.

We further carry out a variety of experiments including (1) the leader’s bandwidth utilization (§6.2.2), (2) latency and network bandwidth usage breakdowns (§6.2.1 and §6.2.2), (3) the cost-effectiveness on bandwidth (§6.2.3), and (4) the time and communication costs of the view-change (§6.2.4). In particular, we scale up both of the two systems to see how their performances, especially the throughput, react with more configured resources at each replica. The evaluation results (see Fig. 11 in §6.2.3) show that, for both of the two systems, the throughput grows proportionally within the moderate available bandwidth (20-200 Mbps). However, the growth rate of throughput in HotStuff approaches to 0 as the protocol scales out, whereas Leopard remains at a high value of about $1/2$ with all tested scales. This indicates that, Leopard benefits a much better cost-effectiveness in practice. We also evaluate the performance of the view change after it has been triggered. The result shows, the time cost is only less than 6 seconds when $n = 400$.

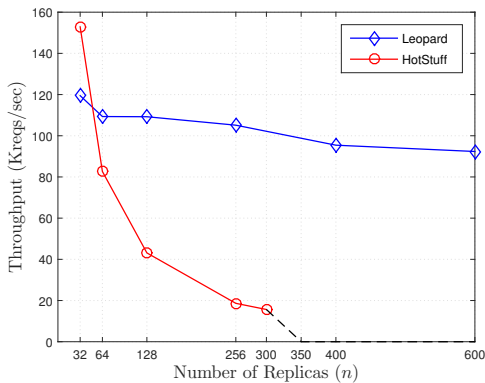


Figure 3: Throughput of our system and HotStuff with a 128-byte payload size.

1.2 Outline

We start by presenting the background and comparison with other related works in §2. The preliminary is presented in §3. The protocol description is in §4, and the analysis is in §5. §6 gives the implementation and four types of experimental evaluations. And the paper is concluded in §7.

2 BACKGROUND & COMPARISON

Reaching consensus in the face of Byzantine failures was first introduced by Lamport, Shostak, and Pease in the 1980s [43, 54]. As a fundamental approach in distributed computing for building fault tolerant systems, it has received numerous attention since then. Classic BFT protocols can provide deterministic safety and liveness via several rounds of voting. The deterministic safety prevents any inconsistency state among replicas which can be exploited by adversaries to cause confusion, fraudulent transactions and distrust [28, 37, 42]. Whereas, deterministic liveness ensures the progress of consensus. The two properties guarantee the security of a resulting fault tolerant system.

Scalability and efficiency have always been the focus when designing a BFT protocol. In recent years, they have become major concerns mostly due to the development of decentralized applications [26, 49, 62]. The first practical BFT protocol in history is the seminal work of PBFT [17]. It guarantees safety and liveness in the partial synchronous network model [24], and this is achieved under the $1/3$ optimal resilience bound [8]. PBFT reaches a consensus by at least two rounds of voting among all replicas via an all-to-all communication pattern. The communication cost of PBFT is $O(n^2)$ during the normal-case mode for confirming a pending request, and $O(n^3)$ during the view-change mode for dealing with a faulty leader. Based on PBFT, improvements on scalability and efficiency have been proposed by a series of works using different ideas, as summarized below.

- *Resilience bound:* BFT protocols are designed to reach consensus under a fraction of Byzantine nodes, a.k.a., the resilience bound. The safety and liveness security properties do not obtain if the resilience bound is violated. Intuitively, the efficiency of a BFT protocol could be improved with a lower resilience bound. To achieve a better efficiency, several BFT protocols [1, 24, 47, 57] relax the resilience bound to a lower value than $1/3$. However, a higher resilience bound means the ability to tolerate a larger number of faults. By contrast, the scalability and efficiency of our protocol is obtained without sacrificing the security which is achieved under the $1/3$ optimal resilience bound.

- *Communication cost:* Reducing the communication cost is a common approach for many PBFT-like protocols to improve both the scalability and efficiency, since the heavy communication cost is a well-known drawback for PBFT. While great efforts have been made on the way to reduce the cost, several recent works [31, 64] use cryptography, especially the threshold signature scheme [11, 12, 22, 59], to allow a single message acknowledgment rather than $O(n)$ messages for each decision. This effectively reduces the communication complexity by one order of n . Experimental evaluations [65] also shown that the scalability and efficiency have been improved significantly, from supporting only tens of replicas as in PBFT to over one hundred, and it can achieve a peak throughput over 10^5 .

Our protocol leverages this idea to obtain a linear communication complexity for the normal-case mode, as well as high efficiency for small scales.

To further simplify the complicated view-change mode of PBFT, a chain-based idea has risen in the past five years where each consensus proposal (e.g., a block) contains a (hash) link to its parent, and the confirmation on one proposal is equivalent to the confirmation on all its preceding proposals. BFT protocols adopting this idea [13–15, 18, 58, 64] reduce the communication cost during the view-change, since only the latest proposal is needed to be synchronized without concerning other preceding ones before starting a new view. However, the drawback is that it requires consensus proposals to get confirmed in a sequential manner, thus losing the ability of the concurrent confirmation which can be beneficial to increase the level of resource utilization as well as efficiency. This is why we give up this idea when presenting the view-change mode. We ensure a concurrently executed agreement during the normal-case mode since it happens most of the time. The communication cost for a view-change in our protocol is the same as LibraBFT [6], the consensus protocol of Facebook’s Diem [4].

- *The number of rounds on voting:* Another idea to improve the efficiency of a BFT protocol is by reducing the number of rounds on voting before an agreement is reached. Following this idea, [31, 41] incorporate a fast path with only one round of voting on top of PBFT, which, however, can be safely used only when no Byzantine replica appears or the network is synchronous. An elegant work of Thunderella [53] combines the classic BFT with blockchain and provides a paradigm such that an agreement can be reached with only one round of voting among replicas. The sacrifice, however, is that it inherits the drawbacks of many blockchain protocols, i.e., the reliance of synchrony and a probabilistic security guarantee (we will talk about it later). In addition, several recent works, HotStuff as a typical example, adopt a pipelining idea [15] to amortize its three-round voting for each agreement over three successive agreement instances. However, [51] has shown that the pipelined version of HotStuff suffers from an attack resulting in about $2/3$ drop of performance. Our protocol achieves an agreement with one less round of voting compared to our closest competitor, HotStuff. Meanwhile, it tolerates the existence of Byzantine replicas and doesn’t rely on synchrony to achieve safety.

After all these efforts, the throughput of existing leader-based BFT protocols still drops significantly when the protocol scales out (see Fig. 1). Therefore, it remains to be an open problem that to design a scalable BFT protocol while preserving high efficiency.

We observed (and verified in experiments) that the neglected but crucial data delivery step is the bottleneck for efficiency when the scale is large since the leader has been stuck. There are several other works [21, 36, 60] notify this. However, no direct solution has been proposed to resolve this problem, only bypassing it via leader-less ones [21, 33, 48, 60]. We first elaborately analyzed and locates the step that gets stuck (§1). We then strive to resolve this via amortizing the cost of the leader by taking full advantage of the idle bandwidth resources of other replicas, which gives us a solution that confronts this problem directly. Experiment shows that our solution is effective.

The idea of amortizing the cost is not new, especially in leader-less BFT protocols where the throughput is contributed by all replicas instead of the leader alone as in leader-based BFT. However, the most efficient leader-less BFT solutions to our knowledge [21, 33, 48] are still hard to provide high efficiency compared to the state-of-the-art leader-based BFT protocols when sticking to the $1/3$ optimal resilience bound.

There are other techniques to balance the workload of a specific node on disseminating messages, for example, the broadcast tree [61] and the erasure code [10]. In the broadcast tree, replicas establish a tree on which each node resides a replica and the sender is on the root. A message is delivered from the root downward layer-by-layer, and each replica only has to deliver the message to its children. However, when all replicas are honest, it still costs $O(\log n)$ time complexity per message delivery. Even worse, this technique is quite susceptible to faults, since any Byzantine node can simply stop passing the message to its children, letting all replicas reside on the subtree rooted by the Byzantine node fail to receive the message. The erasure code is a common technique to even the bandwidth usage and it can tolerate up to $1/3$ Byzantine nodes in an asynchronous network. It is broadly used in the reliable broadcast primitive to reduce the communication cost from quadratic to linear [23, 33, 48]. Compared to ours, this technique requires a larger communication cost both on the leader ($c\Lambda \times \text{payload}$) and the non-leader replica ($c\Lambda \times \text{payload}$), where $\frac{1}{c}$ is the code rate of the erasure code with $c > 1$, e.g., $c = 2$ in the Reed-Solomon code [55]. Besides, it requires an extra computational burden on both the leader for encoding and other replicas for decoding, and this cost grows proportionally to n . Our solution avoids this drawback, thus saving the extra overhead.

Compared to blockchain protocols. Different from the above classic BFT protocols, blockchain protocol, lead by the Nakamoto consensus protocol of Bitcoin [49], can also tolerate Byzantine failures. However, most blockchains [5, 26, 27, 39, 49] can only provide a probabilistic guarantee for both the safety and liveness, rather than deterministic ones as in classic BFT protocols. Besides, they rely on the synchronous network assumption where there is a known message delivery bound Δ . This limitation makes them incapable of the optimistic responsiveness [52] and vulnerable to several attacks [25, 34, 50]. Although the scalability of blockchain is well-achieved, its efficiency is poor. A large number of works try to improve its efficiency. Among these works, Prism [5] presents an excellent blockchain protocol based on Bitcoin by deconstructing blocks to obtain a smaller block size thus shortens the block interval and increases the efficiency. Our protocol is inspired by this technique but with a different purpose. We aim at balancing the workload of replicas and removing the bottleneck of the leader-based BFT protocol. Besides, our protocol is deterministic and doesn’t rely on synchrony.

Furthermore, another promising technique focusing on scalability and efficiency is sharding. By dividing the replicas into several shards such that each shard processing pending requests in parallel, consensus protocols via sharding can achieve a throughput that grows proportionally to the scale of the protocol in principle. Many of the current schemes [3, 40, 46, 67] form a shard by randomly selecting a collection of nodes from the network and each shard

Table 1: Expected error probability when randomly choosing n nodes from network with ρ ratio of faults.

ρn	16	32	64	128	256	400	600
1/4	1.90×10^{-1}	1.54×10^{-1}	5.96×10^{-2}	1.82×10^{-2}	1.30×10^{-3}	8.68×10^{-5}	2.97×10^{-6}
1/5	8.17×10^{-2}	4.11×10^{-2}	5.10×10^{-3}	2.18×10^{-4}	2.44×10^{-7}	1.77×10^{-10}	1.41×10^{-14}

invokes the classic BFT protocol for confirming requests. To protect the security of the BFT protocol, the size of each shard should be large enough to achieve the 1/3 resilience bound with a high probability (see Table 1⁴). Our BFT protocol provides a fundamental component that is scalable and efficient for these sharding schemes. And it can also be recast by the sharding architecture to further get improved. In addition, a recent interesting work of Red Belly [21] uses the sharding technique to reduce verification on the validity of pending requests/transactions. Although this paper focuses on the fundamental consensus protocol like many others [17, 31, 64] without considering the request’s validity which is application-dependent, the same idea of Red Belly can be adopted when our protocol is built to support realistic applications.

3 PRELIMINARY

3.1 Building Blocks

In this part, we introduce definitions for the two signature schemes used in Leopard.

Signature Scheme. A signature scheme contains three algorithms $\mathcal{S} = (\text{KGen}, \text{Sig}, \text{Vrf})$ that works as follows:

- $\text{KGen}(pp) \rightarrow (pk, sk)$. Given a public parameter pp , it outputs a public and private key pair (pk, sk) .
- $\text{Sig}(sk, M) \rightarrow \sigma$. Given a private key sk and message M , it outputs the signature σ on M .
- $\text{Vrf}(pk, \sigma, M) \rightarrow 0/1$. Given the public key pk , signature σ and message M , it outputs 1 if the signature is valid for message M ; otherwise, it outputs 0.

We call a signature scheme is secure iff it satisfies *existentially unforgeable under a chosen-message attack (EUF-CMA)*. Informally speaking, it means that a polynomial-time adversary, who queries $\text{Sig}(sk, \cdot)$ for the signatures of a message set \mathcal{M} chosen by the adversary, cannot produce a valid message and signature pair (M, σ) , where $M \notin \mathcal{M}$.

Threshold Signature Scheme. Let $0 \leq t < n$. A (t, n) -threshold signature scheme contains four algorithms $\mathcal{TS} = (\text{TKGen}, \text{TSig}, \text{TSR}, \text{TVrf})$ as follows:

- $\text{TKGen}(pp, t, n) \rightarrow (tpk, \{tpk_i, tsk_i\}_{i=1}^n)$. Given a public parameter pp , total node number n , and the threshold t of nodes corrupted by adversary, TKGen samples a public

⁴The expected error probability that the requirement of 1/3 resilience bound of byzantine replicas is not satisfied when selecting n replicas from a ratio ρ of byzantine nodes in the network can be estimated by

$$Pr[X > \lfloor \frac{n-1}{3} \rfloor] = 1 - \sum_{l=0}^{\lfloor \frac{n-1}{3} \rfloor} \binom{n}{l} \rho^l (1-\rho)^{n-l}.$$

key tpk , and public and private key pair (tpk_i, tsk_i) of each node $i, i \in \{1, \dots, n\}$.

- $\text{TSig}(tsk_i, M) \rightarrow \sigma_i$. Given a private key tsk_i of node i and message M , it outputs a threshold signature share σ_i .
- $\text{TSR}(pp, R) \rightarrow \sigma/\perp$. Given the public parameter pp and a set R of $t+1$ threshold signature shares, it outputs an aggregated signature share σ if all $t+1$ threshold signature shares are valid; otherwise, it outputs \perp .
- $\text{TVrf}(pp, tpk, \sigma, M) \rightarrow 0/1$. Given the public parameter pp , public key tpk , a threshold signature share (or an aggregated signature) σ and message M , it outputs 1 if the signature is valid for message M ; otherwise, it outputs 0.

We call a (t, n) -threshold signature scheme is secure iff it satisfies two properties: *Unforgeability* and *robustness*. Informally speaking, unforgeability states that a polynomial-time adversary corrupts no more than t nodes, cannot produce a valid aggregated message-signature pair (M, σ) by its own. Whereas robustness states that, if a polynomial-time adversary corrupts no more than t nodes, TKGen and TSig can still complete successfully.

3.2 System Model

We consider a system consisting of a fixed set of $n = 3f + 1$ replicas, indexed by $i \in \{1, \dots, n\}$, where at most f replicas are Byzantine and others are honest. We will often refer to Byzantine replicas as being coordinated and fully controlled by an adversary. Each replica holds two signature key pairs (pk_i, sk_i) and (tpk_i, tsk_i) , where \mathcal{TS} is a $(2f, n)$ -threshold signature scheme. The identities of replicas and their public keys are known to all. The adversary also knows the private keys and internal states of all Byzantine replicas.

Partially synchronous network. Network communication among replicas is point-to-point, authenticated, and reliable. We adopt the partially synchronous network model of Dwork et al. [24], where a known bound Δ on message delivery holds after some unknown time point called the global stabilization time (GST). Time before GST is fully asynchronous with no bound on message delivery, i.e., the adversary can arbitrarily delay. Time after GST is synchronous. This model follows that of many BFT protocols, especially HotStuff [64] and PBFT [17].

3.3 Design goals.

We aim to design a leader-based BFT protocol that preserves high efficiency while scaling out. It should satisfy the following security and efficiency goals under the above-defined threat model.

The security goal. A secure BFT protocol satisfies the following two properties:

- *Safety*: The requests recorded in the same position of two output logs from honest replicas are identical.
- *Liveness*: A client request will eventually get confirmed.

The efficiency goal. The efficiency goal of our protocol is measured by two metrics: optimistic responsiveness and scaling factor.

- *Optimistic responsiveness*: When the leader is honest and after GST, the confirmation latency of a pending request only depends on the actual network delay, rather than any known upper bound of the network delay.

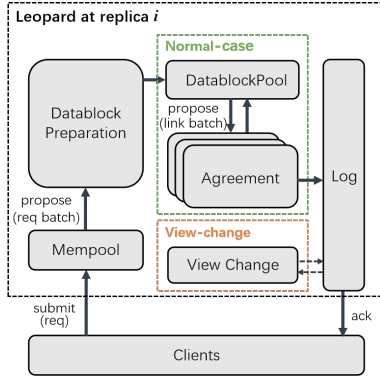


Figure 4: The architecture of Leopard.

- *Scaling factor*: We require that the scaling factor of the protocol, i.e., the heaviest workload on processing per bit among replicas per second when following the protocol, is constant to n .

4 PROTOCOL OF LEOPARD

4.1 Overview

The protocol proceeds in successive views starting from 1, where each view consists of multiple agreement instances and a view-change for advancing to the next view. To preserve a high efficiency while scaling out, we decouple the heavy part of data delivery from the agreement. Fig. 4 depicts the architecture of our protocol that features a memory pool (or *mempool*), a datablock preparation, a normal-case modular to achieve agreements on pending requests, a view-change modular to deal with possible faulty leaders, and a log to store confirmed requests.

The client sends pending requests to non-leader replicas and waits for $f + 1$ identical acknowledgments from replicas as a response. Since there are at most f replicas, a valid response thus contains at least one acknowledgment from honest replicas which ensures the correctness of the response. The typical message flow (corresponds to the solid arrows in Fig. 4) is shown in Fig. 5.

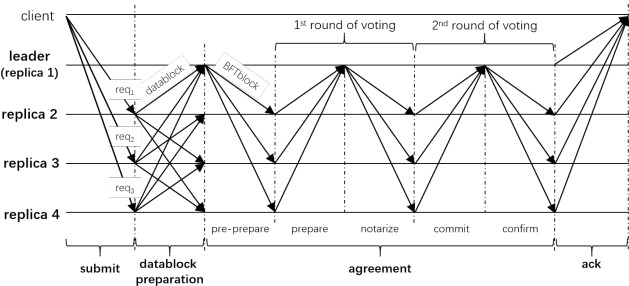


Figure 5: The typical message flow of our protocol with $n = 4$.

Upon receiving requests from the client, each non-leader replica continually packs pending requests from its mempool into datablocks which are sent to all the other replicas. As we try to balance the workload of replicas, we exclude the leader from generating datablocks but leave the responsibility of initiating an agreement

instance to the leader. The leader extracts datablocks, that have been received and passed the basic verification, to generate BFTblocks and sends them to others. Each agreement instance is then to confirm a BFTblock by two rounds of voting.

Since the network is partially synchronous, the received order of messages may not be consistent with the order they sent. Because of this, agreement instances in Leopard are allowed to be confirmed such that even if the former BFTblock has not finished, the latter can be started, and distinct BFTblocks can be concurrently executed instead of sticking to a sequential manner. Meanwhile, to avoid inconsistency of the output logs at different honest replicas, we assign each BFTblock a unique serial number and let the replicas perform a uniqueness verification on each BFTblock before casting a vote. Notice that, every phase in an agreement instance is event-driven on the completion of its prior phase without waiting for any delay. This makes Leopard be responsive in the optimistic case.

As agreement instances are initiated by the leader in a leader-based BFT protocol, a Byzantine leader can obstruct the progress of the protocol by just being silent. We thus need a mechanism to correct this by replacing Byzantine leaders and rebooting the normal-case mode at a new leader, which is just the view-change mode does. It allows the protocol to recover from Byzantine faults and continue to make agreements on requests, thus ensuring the liveness. As in [17, 31], we let the client re-send a timeout request to expose the potential faulty leader to everyone. The difference is that, instead of letting a client broadcast a timeout request to all replicas, we use the datablock to do this job since a datablock will be propagated to all replicas anyway.

4.2 Block Structure

Before presenting the detail of Leopard, we first introduce the two types of new blocks in the protocol: *datablock* and *BFTblock*.

(i) *Datablock*: A datablock is generated by a non-leader replica using requests from its mempool. The formation of a datablock is: $\langle \text{datablock}, \text{header}, \mathcal{R} \rangle$, where \mathcal{R} is a set of requests. Let $\text{header} := \langle (i, \text{dgt}, \text{counter}), \sigma_i \rangle$, where i denotes the identity of its generator, dgt is the digest of \mathcal{R} , counter shows the number of datablocks having been generated by i , and σ_i is a signature by i on the datablock.

(ii) *BFTblock*: The BFTblock is what replicas actually agree on. Each BFTblock gets confirmed by one of multiple *parallel-executed* agreement instances. It is generated by the current leader using datablocks from its datablockPool, but it only contains the links (or hashes) of the involved datablocks. The formation of a BFTblock is: $\langle \text{BFTblock}, (v, sn), ct \rangle$, where v denotes the view number when creating the BFTblock, sn denotes its serial number which is assigned by the leader, and ct represents the content of the BFTblock (i.e., the datablock links). A BFTblock has two states: *notarized* and *confirmed*. A BFTblock is notarized if it has completed the first round of voting, thus a corresponding *notarization proof* exists; a BFTblock is confirmed if it has completed the second round of voting, thus a corresponding *confirmation proof* exists. Replicas change the state of a BFTblock on a valid proof's reception.

4.3 Protocol Description

The protocol is composed of a suite of tiered components to reach consensus on pending requests, among $n = 3f + 1$ replicas in the

partially synchronous network assumption. It outputs a growing log of confirmed requests.

The protocol switches between two modes: the normal-case mode and the view-change mode. The normal-case mode is designed to achieve agreements on pending requests lead by the current view leader. Each view has a unique leader known to all. The view-change mode is designed for replacing Byzantine leaders and advancing to the next view if a faulty leader appears.

We assume the current view number is v and denote the view leader as L_v . We now detail Leopard in a modular way including datablock preparation, normal-case, and view-change.

■ **Datablock preparation.** Datablock preparation is to synchronize pending requests among replicas, completing the delivery of requests before they are being confirmed. To avoid the protocol being stuck at some specific node, all non-leader replicas in Leopard pack pending requests from their mempools and disseminate the generated datablocks to each other. This process occurs on an ongoing basis and proceeds independently at each replica without being disturbed by any other replica, which is for taking full advantage of the network resource of the sender. Algorithm 1 depicts the generation and verification of a datablock. Each datablock contains a counter d indicating the number of datablocks that having been sent at a replica. On receiving a datablock m from replica i , the receiver puts m into its datablockPool if m contains a valid signature from a replica i , and no datablock with a repetitive counter has been received (line 18).

In a large scale environment, geodistributed replicas are likely to receive different pending requests from their neighbor clients, thus the datablock of replica i can be disjoint from the datablock of replica j ($j \neq i$). However, a Byzantine replica may drop a received request to avoid it being confirmed, i.e., censor a specific request. A client is thus allowed to send a request to s (at most $f + 1$) randomly chosen replicas. As less than $n/3$ replicas are Byzantine, a small $s = 9$ is sufficient to obtain an over 99.99% probability that at least one replica is honest, thus the request can be disseminated by the honest one. To identify the replicas responsible to process a given request req , each client can execute a deterministic function $\mu(req)$ that returns s identifiers of replicas. A simple instantiation of $\mu(req)$ is to check: $H(req) \bmod q = H(i) \bmod q$, where $q = \frac{n-1}{s}$. In general, when setting $s = 1$, we can achieve the minimum request delivery repetition, thus the best possible performance.

Remark: We note that, a faulty replica may generate different datablocks with the same d and try to cause an inconsistency among replicas. Considering Leopard is a leader-based BFT protocol, the content of confirmation is decided by the unique leader. Therefore, only the one received by the leader will get confirmed. In addition, by holding two different datablocks with the same counter as an evidence of the equivocation, a punishment mechanism can be adopted to punish i 's malicious behavior. A simple example is to kick replica i out. Moreover, the counter in a datablock can be used to limit the number of datablocks received from a replica, which is a common way of throttling in order to prevent censorship and exhausting the space of numbers.

■ **Normal-case: agreeing on BFTblocks.** We avoid the chain-based structure as in several other BFT protocols [13, 15, 18, 19, 58, 64] to enjoy the parallel agreement, such that multiple agreement

Algorithm 1 Datablock Generation & Verification

```

1: // Datablock generation
2: (for each non-leader replica  $i$ )
3: Init:  $d \leftarrow 1$ 
4: while () do
5:   let  $\mathcal{R}$  be a set of requests extracted from its mempool
6:    $dgt \leftarrow H(\mathcal{R})$ 
7:    $\sigma_i \leftarrow \text{Sig}(sk_i, (i, dgt, d))$ 
8:    $header \leftarrow \langle (i, dgt, d), \sigma_i \rangle$ 
9:    $m \leftarrow \langle \text{datablock}, header, \mathcal{R} \rangle$ 
10:  multicast  $m$  to all replicas
11:   $d \leftarrow d + 1$ 
12:  mempool  $\leftarrow$  mempool  $\setminus \mathcal{R}$     ▶ remove packed requests to avoid
    repetition
13: end while
14: // Datablock verification
15: (for all replicas)
16: upon receiving a datablock  $m$  from replica  $i$ 
17:    $dgt \leftarrow H(m.header.\mathcal{R})$     ▶ check the integrity
18:   if  $(\text{Vrf}(pk_i, m.header.\sigma_i, (i, dgt, m.header.d)) \rightarrow 0) \vee$  (a valid dat-
    ablock with the same  $d$  has been received from  $i$ ) then ▶ verify  $m$ 's
    validity
19:     return reject
20:   else    ▶ the datablock is valid
21:     datablockPool  $\leftarrow$  datablockPool  $\cup \{m\}$ 
22:     return accept

```

instances each carrying a BFTblock can be conducted *concurrently*. We limit the number of parallel-executed BFTblocks to k , in case a Byzantine leader picks a number that is so high that it exhausts all of the possible serial numbers for BFTblocks. Hence, we set a lower watermark lw and a higher watermark $lw + k$ to limit a valid serial number. Since k can be big enough and the parameter lw will be advanced (due to the checkpoint mechanism introduced below), the process of agreeing doesn't stall waiting for the completion of previous BFTblocks, thus the parallel execution will be maintained.

An agreement consists of two-round voting by executing the normal-case protocol (see Algorithm 2). Instead of the all-to-all voting pattern as in PBFT [17] which brings a quadratic communication complexity, we reduce it to linear using the threshold signature scheme. Letting each vote be a threshold signature share generated from TSig algorithm of the threshold signature scheme \mathcal{TS} , a proof can be deduced from the TSR algorithm by inputting sufficient (i.e., $2f + 1$) shares to obtain an aggregated threshold signature result. Since the one who aggregates votes is critical for the completion of an agreement, we let the leader do this job since a faulty leader will be replaced anyway (by the view-change protocol shown below).

In our protocol, BFTblocks are processed (lines 2-40) in parallel. This enables handling new requests without waiting for the completion of previous ones. Since a BFTblock contains links (or *hashes*) to datablocks and a datablock contains requests, the confirmation of a BFTblock is equivalent to the confirmation of all its linked requests. Once a BFTblock is confirmed at replica i , i will store the BFTblock in its local log following the order of m 's serial number. Hence the corresponding requests are also logically stored in the log, where requests linked by a BFTblock can be ordered in alphabetical order.

Algorithm 2 Agreeing on BFTblocks

```
1: Init:  $sn \leftarrow 1; lw \leftarrow 0$ 
2: // Pre-prepare stage
3: (for leader  $L_v$ )
4: let  $ct$  be a set containing the hashes of pending datablocks
5:  $m \leftarrow \langle \text{BFTblock}, (v, sn), ct \rangle$   $\triangleright$  generate a BFTblock  $m$ 
6:  $\sigma_{L_v}^1 \leftarrow \text{TSig}(tsk_{L_v}, H(m))$   $\triangleright$  sign the hash of  $m$  with  $tsk_{L_v}$ 
7: multicast  $(m, \sigma_{L_v}^1)$  to all replicas
8:  $sn \leftarrow sn + 1$ 
9: // Prepare stage
10: (for replica  $i$ )
11: if the received  $(m, \sigma_{L_v}^1)$  satisfies:  $\triangleright$  exclude an invalid BFTblock msg
12: -  $\text{TVrf}(tpk_{L_v}, \sigma_{L_v}^1, H(m)) \rightarrow 1$ ;
13: -  $v$  is the current view number;
14: - no other BFTblock with the same  $sn$  has been voted in view  $v$ ;
15: -  $lw < sn \leq lw + k$   $\triangleright$  limit the outstanding BFTblock number to  $k$ 
16: - each item in  $m.ct$  corresponds to a datablock in its datablockPool;
 $\triangleright$  all linked datablocks have been received and valid
17: then
18:  $\sigma_i^1 \leftarrow \text{TSig}(tsk_i, H(m))$   $\triangleright$  generate  $i$ 's threshold sig share
19: send  $(H(m), \sigma_i^1)$  to  $L_v$   $\triangleright$  first-round vote
20: // Notarize stage
21: (for leader  $L_v$ )
22: wait for  $2f + 1$  valid threshold signature shares for  $H(m)$ 
23:  $\sigma^1 \leftarrow \text{TSR}(\{\sigma_j^1\}_{j=1}^{2f+1})$   $\triangleright$  create the notarization proof for  $m$ 
24: multicast  $(H(m), \sigma^1)$  to all replicas
25: // Commit stage
26: (for replica  $i$ )
27: if  $\text{TVrf}(tpk, \sigma^1, H(m)) \rightarrow 1$  then
28: change the state of  $m$  to notarized
29:  $\sigma_i^2 \leftarrow \text{TSig}(tsk_i, H(\sigma^1))$ 
30: send  $(H(\sigma^1), \sigma_i^2)$  to  $L_v$   $\triangleright$  second-round vote
31: end if
32: // Confirm stage
33: (for leader  $L_v$ )
34: wait for  $2f + 1$  valid signature shares for  $H(\sigma^1)$ 
35:  $\sigma^2 \leftarrow \text{TSR}(\{\sigma_j^2\}_{j=1}^{2f+1})$   $\triangleright$  create the confirmation proof for  $m$ 
36: multicast  $(H(\sigma^1), \sigma^2)$  to all replicas
37: (for replica  $i$ )
38: if  $\text{TVrf}(tpk, \sigma^2, H(\sigma^1)) \rightarrow 1$  then  $\triangleright$  complete the agreement on  $m$ 
39: change the state of  $m$  to confirmed
40: add  $m$  into  $i$ 's log following the order of  $m$ 's serial number
```

When to response the client: As BFTblocks are processed in parallel agreement instances, the order of their confirmations may not follow the order of their serial numbers and the confirmation order at different replicas can also differ. This happens even the leader is honest due to the network model is partially synchronous. However, the execution of requests must follow a sequential order at all replicas. Otherwise, an inconsistent execution state may appear. Thus, only the confirmed BFTblocks (or the linked requests) with sequential serial numbers can be *executed*. According to different the application requirements, there are two options of when to create an acknowledgment to the client: if the request needs a fast response like in the fast payment application, a replica can send an acknowledgment as long as a BFTblock gets confirmed since a confirmed BFTblock will be executed anyway (show in the proof

Algorithm 3 Making a checkpoint

```
1: (for replica  $i$ )
2: let  $sn$  be the serial number of the latest executed BFTblock and  $st$  be the related execution state
3: if  $(sn \bmod k/2 = 0)$  then  $\triangleright$  produce a checkpoint
4:  $cp \leftarrow \langle \text{checkpoint}, sn, H(st) \rangle$ 
5:  $\sigma_i \leftarrow \text{TSig}(tsk_i, cp)$ 
6: send  $(cp, \sigma_i)$  to  $L_v$ 
7: (for leader  $L_v$ )
8: wait for  $2f + 1$  valid checkpoint messages
9:  $\sigma \leftarrow \text{TSR}(\{\sigma_j\}_{j=1}^{2f+1})$   $\triangleright$  create a proof for  $cp$ 
10: multicast  $(cp, \sigma)$  to all replicas
11: (for replica  $i$ )
12: if  $\text{TVrf}(tpk, \sigma, cp) \rightarrow 1$  then
13: update the maintained latest checkpoint message  $lc$  to  $(cp, \sigma)$ 
14:  $lw \leftarrow sn$   $\triangleright$  advance the lower water mark  $lw$ 
15: return accept
```

for safety); otherwise, if the client needs to know the final execution state, the acknowledgment can only be created until the BFTblock having been executed.

Remark: A missing datablock may induce an insufficient vote since a replica should check whether all linked datablocks in m have been received (line 16) before casting the first-round vote. This issue can be resolved by letting the replica request the missing ones to others. Since the leader has proposed a BFTblock containing the hash of a datablock, the leader must have received the linked datablock. Hence, at least the honest leader will respond to a missing request. The leader-follower architecture, a common software model in database systems [35] where the leader communicates with its multiple followers to assign and integrate works, can further be used to deal with these requests in parallel without impeding the agreement process of the leader;

Since we focus on the consensus of pending requests like many other BFT solutions [17, 48, 64], there is no verification of the request's validity presented in the current protocol. When the protocol is applied to some application scenarios, an application-specific verification function `verify()` is required before casting the first round of voting. Since every datablock containing pending requests has to be received before the vote in the protocol, the verification can be directly added. Meanwhile, similar to [21], conflicting requests in different datablocks can be marked by the leader before a datablock being linked by a BFTblock. This will not add any extra workload since each request should be verified by `verify()` anyway.

■ **Normal-case: making checkpoints.** To reduce the storage overhead, a.k.a., do the garbage collection, when a BFTblock has been executed, we can remove all executed requests from the buffer which are logically linked in a BFTblock with a lower serial number. As in [17, 31], we periodically (every $k/2$) invoke a checkpoint protocol on the latest executed BFTblock B . The generation of a valid checkpoint is a one-round voting process. Thereafter, the messages related to every BFTblock with a serial number lower than B 's can be removed from the buffer. Meanwhile, we advance the lower watermark lw in Algorithm 2 to the serial number of B . The generation of a checkpoint is presented in Algorithm 3.

■ **View-change: replacing Byzantine leaders.** The view-change protocol aims to replace Byzantine leaders and reboot the normal-case mode at a new leader in the next view. It contains three steps: view-change trigger, leader rotation, and state synchronization. View-change trigger decides when to do a view-change. Leader rotation appoints the new leader. State synchronization synchronizes the state and BFTblocks of the current view in order to avoid conflicts in the new view with a new leader.

We adopt a simple round-robin policy as in [19, 31, 38] for the leader election, where the $(v \bmod n)$ -th replica is the eligible leader of view v . The view-change trigger and state synchronization steps are as follows:

- *View-change trigger:* A client randomly selects s replicas (as stated in the datablock preparation) and re-sends a timeout request to the chosen replicas, in which the honest replica will propagate the request (with a special tag) in a datablock. A replica starts a timer when it receives a re-sent request, either from the client or inside a datablock from another replica. The replica i triggers a view change either (1) a timer expires and no acknowledgment of the request have been sent, and in this case, i sends a timeout message $\langle \text{timeout}, v \rangle$, together with i 's signature on it, to all replicas, or (2) i receives a proof that the leader is faulty either via a publicly verifiable contradiction or when received $f + 1$ timeout messages from other replicas. The replica then stops executing the normal-case protocol (Algorithm 2 and 3) of the current view v .

- *State synchronization:* Each replica i collects all notarized BFTblocks with a serial number higher than lw . Replica i sends a view-change message $m = \langle \text{view-change}, v + 1, lc, \mathcal{B} \rangle$, together with i 's signature on m , to the leader of the next view $v + 1$. \mathcal{B} is a set containing hashes of collected BFTblocks and their notarization proofs.

The next view leader L_{v+1} waits for $2f + 1$ valid view-change messages. L_{v+1} then multicasts a new-view message $\hat{m} = \langle \text{new-view}, v + 1, \mathcal{V} \rangle$, together with L_{v+1} 's threshold signature on \hat{m} , to all replicas. \mathcal{V} is the set of $2f + 1$ view-change messages.

When a valid view-change message is received, such that it is signed by the eligible leader and contains $2f + 1$ valid new-view messages, i advances to view $v + 1$. Replicas restart the normal-case mode under view $v + 1$ by first redoing the agreement for each BFTblock linked in \mathcal{V} without re-executing them. The empty position between BFTblocks is filled with a dummy BFTblock with empty content.

Remark: Like PBFT, the state synchronization during a view-change needs to resolve every BFTblock after lw with a maximum of k BFTblocks. This is due to there are at most k BFTblocks processed in parallel. While in the works adopting the chain-based idea as we compared in §2, the cost on state synchronization is limited to the latest BFTblock rather than a k length window of BFTblocks since there is at most one BFTblock being processed simultaneously. It seems to be a tradeoff between higher parallelism and a lower view-change cost. Meanwhile, the decoupling of data delivery and the proposed mechanism in the above can also be leveraged based on chain-based BFT protocols, like HotStuff [64], to preserve the efficiency while the number of replicas increases.

5 ANALYSIS

5.1 Security Analysis

The protocol satisfies safety, captured in Theorem 5.3, and liveness, captured in Theorem 5.4. We first give and prove Lemma 5.1 and Lemma 5.2 before presenting the proof of safety.

LEMMA 5.1 (UNIQUENESS). *Assume the threshold signature scheme is secure. If two BFTblocks B_1 and B_2 both with the same serial number are notarized in the same view, then it must be the case that $B_1 = B_2$.*

PROOF. Since B_1 is notarized and by the definition of the protocol, there must be a set R containing $2f + 1$ distinct replicas who have signed B_1 ; otherwise, a reduction can be built to break the unforgeability of the threshold signature scheme. As there is at most f Byzantine replicas, at least $f + 1$ honest replicas are contained in R . Similarly, we have that at least $f + 1$ honest replicas have signed B_2 . Since there are $3f + 1$ replicas in total and by the pigeon-hole principle, at least one honest replica has signed both B_1 and B_2 . Since an honest replica will only sign one BFTblock with a specific serial number, it holds that $B_1 = B_2$. □

LEMMA 5.2. *For any serial number sn , if any two honest replicas have two BFTblocks with the serial number equals to sn in their output logs, the contents of the two BFTblocks are the same.*

PROOF. We denote the two BFTblocks from the two honest replicas' logs as B and B' , respectively. Due to Lemma 5.1, if B and B' are added into the logs in the same view, then it holds $B = B'$. We now consider the case that they are added into the logs in different views v and v' , respectively. W.l.o.g., we assume $v < v'$.

Following Algorithm 2 (line 40), B (resp. B') is added into the log in view v (resp. v') since it gets confirmed. Hence, there must be $2f + 1$ replicas knows that B (resp. B') is notarized. If the serial number of B is lower than the lower watermark lw , the execution state after B has been included in the latest checkpoint message. Hence, an honest replica will never accept a different BFTblock from B with the serial number sn following Algorithm 2 (line 15). Otherwise, since the new-view message for advancing to view v' contains $2f + 1$ view-change messages and there are at most f Byzantine replicas, at least one honest replica i satisfies (1) B is notarized at i , and (2) the new-view message contains the view-change message from i . Hence, the protocol will redo the B in view v' with the same serial number sn , only with a new view number v' . Hence, the contents of B and B' remains the same. □

THEOREM 5.3 (SAFETY). *Assume the hash function is collision-resistant. If two distinct requests exist on the same position of two output logs, then the two logs cannot be both from honest replicas.*

PROOF. Since a BFTblock contains links to datablocks and each datablock contains requests, Theorem 5.3 follows directly from Lemma 5.2. □

Due to the FLP impossibility [29], the liveness of Leopard relies on the synchronous assumption, where synchrony is achieved after GST in the standard partially synchronous network model adopted in this paper.

THEOREM 5.4 (LIVENESS). *After GST, the confirmation for a pending request must be completed.*

PROOF. In the optimistic case that both the leader and the replica i who receives a pending request req from the client are honest, the leader will link the datablock sent by i , which contains req , into a BFTblock. After a period of another 5Δ , the BFTblock that logically links req will be confirmed hence req gets confirmed too.

If the replica i is faulty and it ignores req , the client will re-send req to at most $f+1$ replicas within which at least one honest replica exists who will disseminate req in a newly generated datablock to all replicas including the leader. This then reduces to the optimistic case in the above.

If the leader is faulty and it ignores datablocks containing req when generating a BFTblock, the re-sent request will trigger a view-change due to the timeout mechanism in the view-change protocol. Since there is at most f Byzantine replicas, after at most another $f-1$ new views, there must be a view with an honest leader. This then reduces to the above case. \square

5.2 Efficiency Analysis

Now we analyze the two main efficiency goals of our protocol, namely scaling factor and optimistic responsiveness, as well as the cost-effectiveness of the protocol.

Recall that, the optimistic responsiveness requires that the confirmation latency of a pending request only depends on the actual network delay δ rather than any known upper bound of the message delay when the current leader is honest and after GST. The protocol is optimistic responsiveness because there is no waiting for any extra delay during the confirmation. It is in essence event-driven as depicted in Algorithm 2 and Fig. 5. Assuming that a client sends a request req to replicas at time t , all honest replicas will confirm req at time $t+7\delta$ if the leader follows the protocol after GST. As in PBFT, it requires that the timer for triggering a view-change should be set appropriately to avoid switching to a new view due to a natural network delay in the optimistic case.

Next, we analyze the scaling factor of our protocol. To simplify the analysis, we first focus on the heavy part of data delivery for initiating the agreement. In the best case that all replicas follow the protocol and datablocks are disjoint, the pending requests are propagated by $n-1$ non-leader replicas and each replica contributes $\frac{\Lambda}{n-1}$ bits where Λ denotes the total bits of requests processed by the protocol per second.

Let α be the number of bits in a datablock, and β be the size of a hash output. Since a BFTblock only contains the hashes of datablocks, we have that the size of the BFTblock for dealing with Λ bits can be estimated by $\frac{\Lambda}{\alpha} \times \beta$.

Hence, the leader's workload per second is estimated by,

$$\begin{aligned} \Gamma_1 &= \Gamma_{\text{leader}}^{\text{send}} + \Gamma_{\text{leader}}^{\text{recv}} \\ &= \frac{\Lambda}{\alpha} \times \beta \times (n-1) + \frac{\Lambda}{n-1} \times (n-1) \\ &= \Lambda \times \frac{\beta(n-1)}{\alpha} + \Lambda, \end{aligned} \quad (3)$$

where $\Gamma_{\text{leader}}^{\text{send}}$ represents the workload per second for generating and disseminating BFTblocks to other $n-1$ replicas, and $\Gamma_{\text{leader}}^{\text{recv}}$ represents the workload per second for dealing with datablocks received from other $n-1$ replicas.

The workload of each non-leader replica per second is,

$$\begin{aligned} \Gamma_2 &= \Gamma_{\text{non-leader}}^{\text{send}} + \Gamma_{\text{non-leader}}^{\text{recv}} \\ &= \frac{\Lambda}{n-1} \times (n-1) + \\ &\quad \frac{\Lambda}{n-1} \times (n-2) + \frac{\Lambda}{n-1} + \frac{\Lambda}{\alpha} \times \beta \\ &= 2\Lambda + \frac{\Lambda}{\alpha} \times \beta. \end{aligned} \quad (4)$$

$\Gamma_{\text{non-leader}}^{\text{send}}$ represents the workload per second for generating datablocks and disseminating pending requests in datablocks to other $n-1$ replicas. $\Gamma_{\text{non-leader}}^{\text{recv}}$ represents the workload per second for (1) receiving datablocks from other $n-2$ replicas, (2) receiving pending requests from the client, and (3) receiving BFTblocks from the leader.

From the above, we have that the scaling factor, i.e., the heaviest workload at an honest replica on processing per bit per second is,

$$\begin{aligned} SF &= \max\{\Gamma_1, \Gamma_2\} / \Lambda \\ &= \max\left\{\frac{\beta(n-1)}{\alpha} + 1, 2 + \frac{\beta}{\alpha}\right\}. \end{aligned}$$

Notice that, α is a system parameter denoting the datablock size. When we set $\alpha = \lambda(n-1)$ where λ is a constant positive number, then SF is constant to n .

A natural consideration is that, since each replica should disseminate datablocks to other $O(n)$ replicas and the size of a datablock $\alpha = O(n)$, it seems that the protocol has a $O(n^3)$ communication cost. We mention that, each replica processes $\frac{\Lambda}{n-1}$ bits, which are then sent to $n-1$ other replicas. The protocol's total number of bits costed (or the bit complexity) in the data delivery is $n \times \frac{\Lambda}{n-1} \times (n-1) = n \cdot \Lambda$. We note that, no protocol can achieve a lower cost since every replica should at least receive all pending bits which already costs $n \cdot \Lambda$.

Next, we deal with the cost after the agreement has been initiated. Notice that the cost is mainly for the two-round voting, and we assume a vote size is γ . Since there are $\frac{\Lambda}{\alpha}$ datablocks when dealing Λ bits of requests and each BFTblock containing at least one datablock, we have that the cost on receiving votes by the leader is at most $\frac{\Lambda}{\alpha} \times 2\gamma \times (n-1)$. Each non-leader replica only has to send/receive one vote message during the agreement because of the usage of threshold signature in our protocol. Due to $\alpha = \lambda(n-1)$, we have that the cost at each replica on dealing with the votes is also constant to n .

Following the above, we can deduce that the workload processing per bit at any honest replica is a constant value that irrelevant to n . Therefore, the scaling factor of our protocol is constant, which achieves the efficiency goals.

Now we give an analysis of the cost-effectiveness when scaling up the protocol. Notice that, the performance of the protocol can be effectively improved by adding resources like CPU and bandwidth implies that, there should be no fixed delay between messages' processing in the protocol. This means the protocol should feature the hallmark of responsiveness. Since Leopard is optimistic responsiveness, its performance can be effectively improved by adding resources at each replica in the optimistic case when the leader is honest.

Let Λ^Δ denote the increased bits of requests processed per second by the protocol, and W^Δ denote the heaviest increasable workload on processing pending requests per second among replicas. When $\beta < \lambda$, we have that $\frac{\beta(n-1)}{\alpha} < 1$. Notice that $\alpha = \lambda(n-1)$ and $n \geq 2$, thus $\beta < \alpha$. From Eq. (3) and (4), we deduce that

$$\begin{aligned} \frac{\Lambda^\Delta}{W^\Delta} &= \Lambda^\Delta / \max\{\Gamma_1^\Delta, \Gamma_2^\Delta\} \\ &= \Lambda^\Delta / \max\{\Lambda^\Delta \times \frac{\beta(n-1)}{\alpha} + \Lambda^\Delta, 2\Lambda^\Delta + \frac{\Lambda^\Delta \times \beta}{\alpha}\} \\ &= 1 / \max\{\frac{\beta(n-1)}{\alpha} + 1, 2 + \frac{\beta}{\alpha}\} \\ &= \frac{1}{2 + \frac{\beta}{\alpha}}, \end{aligned}$$

which is about 1/2.

6 IMPLEMENTATION & EVALUATION

6.1 Implementation

We have implemented a prototype of Leopard in Golang within roughly 5,600 lines of code. The system architecture is illustrated in Fig. 6. We implement a *modular* BFT system and extract the mechanisms for ensuring safety and liveness to encapsulate the normal-case protocol and view-change protocol.

Functionally the protocol can be divided into seven modules shown in Fig. 6. The execution engine is to pass a newly received message to the related modules for verification and casts a vote on valid messages. The block manager is mainly for verifying the validity of blocks with the help of cryptographic algorithms provided by the crypto toolkit. The block pool is to store outstanding blocks. The log manager records confirmed requests. The view transfer is to trigger a view-change and advance to a new view. The reliable and authenticated channel is for delivering messages to/from others.

Since a high throughput and a large scale of replicas are expected, there is a large quantity of message exchanges. To avoid a frequent handshake during the message delivery which can affect the performance, we realize the communication channel by a point-to-point HTTP persistent connection based on TCP [63]. Moreover, we notice that the heaviest part of the communication lies in the delivery of datablocks, but the one that determines the confirmation is the messages related to BFTblocks. We use two channels in Golang to deal with BFTblocks (channel ①) and datablocks (channel ②) as shown in Fig. 6, respectively. To avoid the congestion from datablocks, we set channel ① with a higher priority than channel ②. It ensures the progress of the agreement.

6.2 Experimental Evaluation

In this part, we show that Leopard supports at least 600 replicas. Meanwhile, it preserves a high efficiency and reaches about 10^5 throughput for all tested scales. We compare the performance of Leopard to HotStuff, its closest competitor, using the implementation by its authors [66]. Since the verification cost of a pending request in diverse application environments differs and we mainly focus on the consensus, we only evaluated the performances of both systems without any extra application-specific verification.

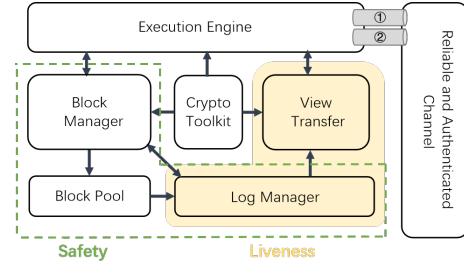


Figure 6: Architecture of Leopard implementation.

There are other implementations of BFT solutions such as BFT-SMaRt [9], Tendermint [13] and SBFT [31]. To save the cost for large-scale experiments, we only conducted experiments with the state-of-the-art solution, HotStuff.

We ran four types of experiments, all with a Byzantine replica number to the largest possible one (i.e., touching the 1/3 optimal resilience bound) to confirm the performance with the highest achievable fault tolerance:

- (i) we varied the number of replicas up to 600 to evaluate the scalability of both systems (§6.2.1);
- (ii) we evaluated leaders' bandwidth costs of both systems (§6.2.2);
- (iii) we varied the configured bandwidth on each replica to evaluate the cost-effectiveness of both systems (§6.2.3);
- (iv) we further evaluated the time and communication costs on the view-change part of Leopard (§6.2.4).

The experiments were conducted on Amazon EC2 virtual machine (c5.xlarge) instances, each has 4 vCPUs and a 4.9 Gbps to 9.8 Gbps TCP bandwidth measured by *iperf* among several randomly selected instances. We ran each replica on a single EC2 instance. All the EC2 instances are connected via a point-to-point network. Every experimental result below is averaged over 3 runs, each lasting until measurements stabilized in that run.

6.2.1 Scalability. To compare the scalability of Leopard and HotStuff, we examed the throughput and latency of the two systems with a fixed 128-byte payload size and an increasing number of replicas. This shows how fast they could go. By default, the throughput is measured by the leader. We measured the latency as the time elapsed from the client submitting the request until it has received $f + 1$ valid responses. This measurement of latency captures the time used for a request from its generation to its finalization, which is a full path with no other measurement that leads to a longer result. Since the leader in both systems generates the confirmation proof and then deliveries the proof to other replicas, the leader will output a confirmation ahead of other replicas. This seems that the throughput measured from the leader maybe a little bit higher than from other replicas at some point in time. However, our evaluation result is an average of several runs each was collected when the system had been stabilized. We observed that the results measured from the leader and an honest replica are almost the same.

Intuitively, increasing the batch size of consensus proposals (i.e., BFTblock), denoted as *BFTsize* below, can better amortize the cost and leads to a higher throughput regardless of the latency for a fixed n . Besides, the batch size of a datablock, i.e., the number of requests per datablock which denoted as *datablock size* below, in

Leopard should be set with a larger value to counteract the effect due to an increasing n .

Therefore, we first measured the results on varying the two batch sizes (i.e., BFTsize and datablock size) with a varying number (32-600) of replicas. Notice that in HotStuff, as well as most other BFT solutions, there is only one batch and it is for batching requests into a consensus proposal (i.e., a block) directly. Fig. 7 depicts the throughput with different batch sizes for five replica numbers (32, 64, 128, 256, 300) in HotStuff. Results show that throughput goes up as we increase the batch size, but it stops growing after a certain batch size value. We let the batch size at this point be the implementation parameter of HotStuff. We remark that, the latency still goes up if we keep increasing the batch size. As for Leopard, we varied one bath size while fixing the other one for six replica numbers (32, 64, 128, 256, 400, 600). Fig. 8 depicts the throughput and latency of Leopard with different datablock sizes and BFTsizes when $n = 64$ as an example. We use a red box in Fig. 8 to show the batch size we choose after balancing the throughput and the latency. Since the results with other n values present a similar tendency to $n = 64$, we omit the experimental results.

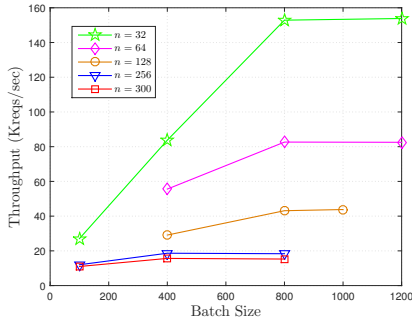


Figure 7: Throughput of HotStuff on varying batch sizes.

The results above show that the increase of BFTsize does not help to increase throughput after a certain value, but the latency keeps increasing. It confirms that the throughput cannot be improved just by setting a larger batch size, and this is consistent with the experimental results in other works [13, 21, 65]. Also, both the throughput and the latency keep increasing as datablock size getting larger. However, after a certain value, the increased latency becomes significantly larger than the increased throughput. The resulting implementation parameters⁵ are listed in Table 2. The experiment below is conducted with the resulting implementation parameters.

Fig. 9 depicts throughput (left figure) and latency (right figure) of Leopard and HotStuff. Since the current HotStuff implementation can hardly work when $n > 300$, we only show the results of HotStuff with n up to 300. It shows that the throughput of Leopard drops only slightly and remains almost flat when n varies up to 600. Compared to HotStuff, Leopard achieves a 5× throughput when $n = 300$ and the gap gets wider with an increasing n . The latencies of both systems share the same tendency as n increases. However,

⁵The datablock size in this section represents $\frac{\alpha}{\text{payload}}$, where α is the total number of bits in a datablock and payload is the number of bits per request. We note that the analysis of Leopard in §5.2 used α to estimate the workload of replicas, and payload is 128 bytes in our experiment.

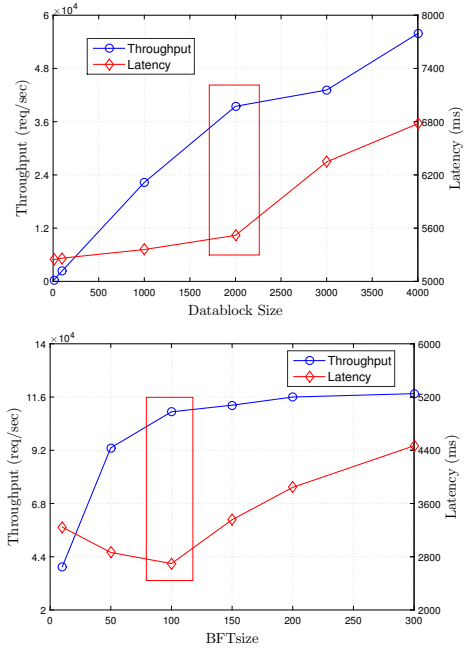


Figure 8: Performance of Leopard on varying batch sizes with $n = 64$.

Table 2: Implementation parameters.

n	Batch sizes in Leopard		Batch size in HotStuff
	datablock size	BFTsize	
32	2000	100	800
64	2000	100	800
128	3000	300	800
256	4000	300	800
300	–	–	800
400	4000	400	–
600	4000	400	–

the latency of Leopard is higher than HotStuff for all tested n . This is because, when following the implementation parameters in Table 3, the number of requests processed by a BFTblock (i.e., datablock size × BFTsize) in Leopard is larger than the number processed per block in HotStuff. Hence, Leopard spends a longer time collecting enough requests. HotStuff avoids this problem since no datablock decoupled from the consensus proposal. However, the throughput of HotStuff drops significantly while scaling out which makes it suffer from the scalability-efficiency dilemma. In spite of that, the latency of Leopard is good when the scale is small (e.g., less than 1.5 seconds with $n \leq 32$).

To further evaluate the latency, we broke the latency down and measured the usage of time on different steps during an agreement in Leopard’s implementation. The result in Table 3 shows that, Leopard’s implementation costs over 60% on the datablock preparation. In particular, over 50% is spent on the datablock delivery. This means that datablock delivery dominates the latency. This indicates the correctness of our design concept, i.e., to allow replicas disseminating datablocks on an ongoing basis without being impeded by each other which makes full use of the resource.

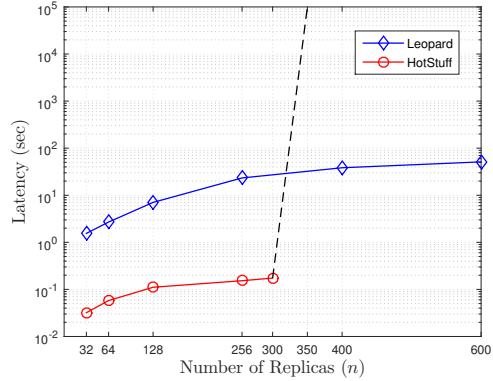
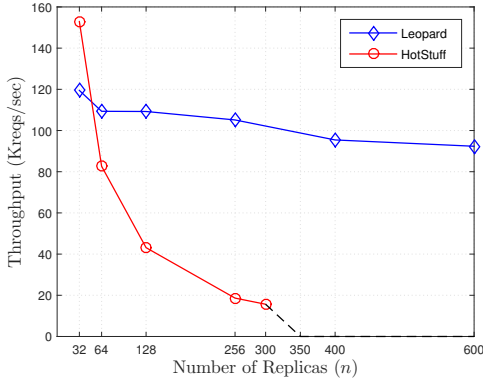


Figure 9: Scalability of Leopard and HotStuff.

Table 3: Latency breakdown of Leopard’s implementation with $n = 32$.

Usage		%Latency
Datablock Preparation	Datablock Generation	12.98%
	Datablock Delivery	50.30%
	SUM	63.28%
Agreement		35.97%
Response to the Client		0.75%

To mitigate the latency increase, we can set a short-timer, such that if the timer expires, an agreement instance will be started with all collected requests, rather than waiting for enough requests as before. Also, the vote in Leopard’s implementation is instantiated by the BLS threshold signature [12], whereas other signatures in Leopard and all signatures and votes in HotStuff are instantiated by ECDSA with secp256k1. Since there is a $200\times$ time cost in BLS (10 ms) compared to ECDSA with secp256k1 ($50\ \mu\text{s}$) for each signature verification, the instantiation of the threshold signature in Leopard also contributes to the latency gap. We note that various engineering optimizations, such as parallel TCP connections or more aggressive TCP congestion control strategies [16] and parallelization for validating burst incoming data, can further optimize current Leopard’s implementation. We leave it as our future work.

6.2.2 Leader’s Overhead. As state in §1, the leader’s overhead is the major bottleneck of the scalability and efficiency in existing leader-based BFT protocols. We evaluate the leader’s bandwidth utilization for both Leopard and HotStuff and the result is depicted in Fig. 10. It shows that the leader’s bandwidth usage in Leopard has been greatly reduced to an acceptable value much lower than 0.5 Gbps. Also, it remains almost flat and it is much lower than HotStuff whose leader’s bandwidth usage rises rapidly with an increasing n .

We also evaluate the bandwidth usage breakdown at both the leader and non-leader replica in the Leopard’s implementation. Table 4 presents the evaluation result when $n = 32$. It shows that most of the bandwidth (over 96%) of the leader is used on receiving datablocks, whereas the cost of sending consensus proposals is only 3.17%. For each non-leader replica, most of the bandwidth is used on sending/receiving datablocks and the cost of sending is a little bit higher than the cost on receiving. This is due to that a replica sends

a datablock to all $n-1$ others but receives datablocks from $n-2$ other replicas (since the leader is excluded from generating the datablock). Notice that, the bandwidth used on receiving pending requests (both from other replicas and clients) takes up about 50% of the total bandwidth usage at a non-leader replica. Since the achievable throughput is limited by the number of requests received per second, this indicates that the effective network bandwidth utilization ratio, i.e., confirmed bits per second over the configured bandwidth, is $1/2$ in our protocol. Moreover, we further notice that just a very small percentage (less than 1%) of bandwidth is costed on dealing with votes. This confirms that using vote-complexity to measure the efficiency of a leader-based BFT protocol as in previous works is defective.

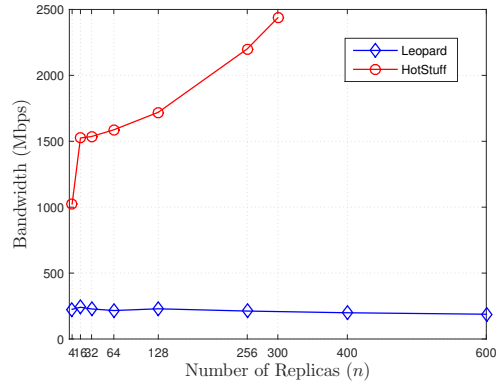


Figure 10: Bandwidth utilization of the leader in Leopard and HotStuff.

6.2.3 Cost-effectiveness. A common way in practice to make a system perform better is to configure with more physical resources, a.k.a, scaling up in a distributed system. A natural question is: whether the scalability-efficiency dilemma can be mitigated or even conquered by configuring with more bandwidth resources. We evaluate how Leopard and HotStuff perform with an increasing available bandwidth at each replica.

We thus throttled the available bandwidth at each replica from 20 Mbps to 200 Mbps using NetEm [45]. Fig. 11 depicts throughput under different available bandwidths at each replica, for both Leopard

Table 4: Network bandwidth usage breakdown of Leopard’s implementation with $n = 32$.

Role	Usage		%Bandwidth
Leader	Sent	Consensus Proposal	3.17%
		Vote Result/Proof	0.24%
		Miscellaneous	0.15%
		SUM	3.56%
	Received	Datablock	96.17%
		Vote	0.16%
Miscellaneous		0.10%	
SUM	96.44%		
Non-leader Replica	Sent	Datablock	49.93%
		Vote	0.01%
		Miscellaneous	0.05%
		SUM	49.99%
	Received	Consensus Proposal	0.05%
		Datablock	48.34%
		Vote Result/Proof	0.01%
		Reqs. from Clients	1.61%
		SUM	50.01%

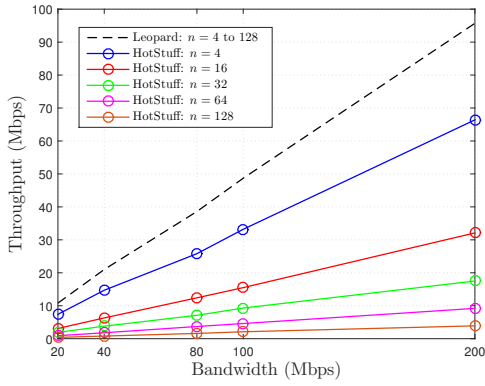


Figure 11: Throughput with different available bandwidths at each replica in Leopard and HotStuff.

and HotStuff with a varying n . It shows that for both systems and all tested n , the throughput scales proportionally with the available bandwidth. Therefore, the throughput of both Leopard and HotStuff can be improved by configuring with more bandwidth resources. However, when n becomes larger, the ratio of increased throughput over the increased bandwidth approaches to 0 in HotStuff. This means that the throughput of HotStuff cannot be improved effectively under a large n . Hence, configuring with more bandwidth resources cannot resolve its scalability-efficiency dilemma. As a comparison, the effective network bandwidth utilization ratio of Leopard remains at about 1/2. This is consistent with the result of network bandwidth breakdown in §6.2.2. As it is significantly superior to HotStuff with all tested n values, Leopard is more cost-effective on the available bandwidth than HotStuff.

To confirm our analysis in §1 about the $\frac{1}{n-1}$ effectiveness when scaling up the HotStuff, we recast the experimental result in Fig. 11 and show it together with the theoretical result analyzed above in Fig. 12. As we can see, the experimental result is almost consistent with our theoretical result, i.e., $\frac{1}{n-1}$. We note that the gap between theoretical and evaluation results, especially when n is less than about 32, is mainly due to that, a portion of bandwidth is used on

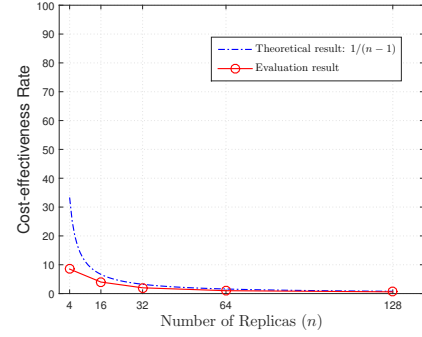


Figure 12: The cost-effectiveness of HotStuff with a varying n .

receiving requests from clients which we omit in our calculation to deduce $\frac{1}{n-1}$ for a better understanding. The gap narrows with n increases since the throughput drops.

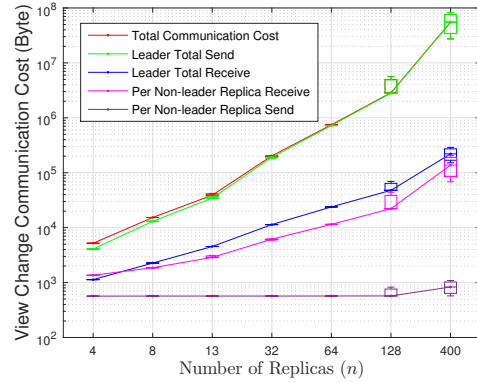
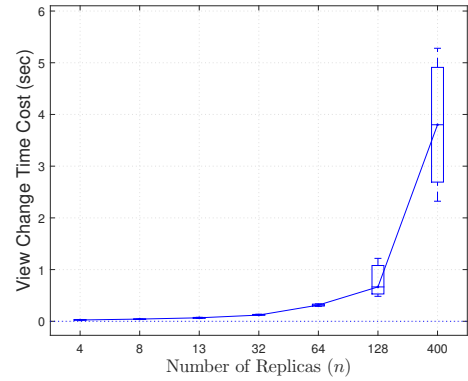


Figure 13: View-change time and communication costs of Leopard’s implementation.

6.2.4 View Change. To evaluate the performance of a view-change in Leopard, we examined the time and communication costs with up to 400 replicas after the view-change has been triggered. To this end, we randomly stop the leader to trigger a view-change.

Fig. 13 depicts the results on measuring the time cost (left) and communication cost (right) with a varying n after a view-change

has been triggered. It shows that, when the protocol scales up, both the time and total communication cost will increase. However, when the protocol scale goes up to hundreds (400), the time cost on a view-change state synchronization period can be still in seconds (less than 6s). We note that the cost on a view-change after it has been triggered is mainly for processing BFTblocks not included in the latest checkpoint. Since the number of requests processed per BFTblock (i.e., datablock size \times BFTsize) in Leopard is large, the number of outstanding BFTblocks is small during a view-change, compared to others like PBFT. This leads to less cost during a view-change in Leopard. Besides, it shows that the total communication cost of the protocol overall during a view-change is mainly from the leader. This is due to that the leader should distribute a new-view message containing $2f + 1$ view-change messages to all the others. In addition, we find out that, the resulting gap from each run increases as n getting larger. This is due to that we triggered a view-change randomly in this experiment, which makes the number of outstanding BFTblocks vary.

7 CONCLUSION

The scalability and efficiency are two key metrics for a practical BFT protocol, especially due to the emergence of decentralized applications. However, the throughput of existing leader-based BFT protocols drops significantly when the protocol scale increases. They thus face a scalability-efficiency dilemma. In this paper, we analyzed the bottleneck to this problem and defined a new metric called “scaling factor” to capture whether a BFT protocol will preserve the efficiency when the number of replicas increases. We next presented a BFT protocol called “Leopard”. Our protocol enables preserving the high throughput while the scale increases, and it has a scaling factor constant to n which is desirable. This is achieved by amortizing the workload of the leader adaptively to the number of replicas by taking full advantage of the idle resources of other replicas. We conducted a variety of experiments on our implementation of Leopard with up to 600 replicas. The evaluation shows the throughput of Leopard remains almost flat at 10^5 and also significant multi-sided performance improvements to the state-of-the-art BFT solution, HotStuff.

ACKNOWLEDGEMENTS

We would like to thank the anonymous reviewers from IEEE S&P 2021 of the winter quarter submission for their valuable comments.

REFERENCES

- [1] Michael Abd-El-Malek, Gregory R. Ganger, Garth R. Goodson, Michael K. Reiter, and Jay J. Wylie. 2005. Fault-Scalable Byzantine Fault-Tolerant Services. In *Proceedings of the Twentieth ACM Symposium on Operating Systems Principles (SOSP '05)*. ACM, 59–74.
- [2] Yair Amir, Brian A. Coan, Jonathan Kirsch, and John Lane. 2011. Prime: Byzantine Replication under Attack. *IEEE Trans. Dependable Secur. Comput.* 8, 4 (2011), 564–577.
- [3] Elli Androulaki, Christian Cachin, Angelo De Caro, and Eleftherios Kokoris-Kogias. 2018. Channels: Horizontal Scaling and Confidentiality on Permissioned Blockchains. In *Computer Security*. Springer, 111–131.
- [4] Diem Association. 2021. The Diem: To build a trusted and innovative financial network that empowers people and businesses around the world. <https://www.diem.com/en-us/>. (2021).
- [5] Vivek Bagaria, Sreeram Kannan, David Tse, Giulia Fanti, and Pramod Viswanath. 2019. Prism: Deconstructing the Blockchain to Approach Physical Limits. In *Proceedings of the 2019 ACM SIGSAC Conference on Computer and Communications Security (CCS '19)*. ACM, 585–602.
- [6] Mathieu Baudet, Avery Ching, Andrey Chursin, George Danezis, François Garillot, Zekun Li, Dahlia Malkhi, Oded Naor, Dmitri Perelman, and Alberto Sonnino. 2019. State Machine Replication in the Libra Blockchain. *The Libra Assn., Tech. Rep* (2019).
- [7] Johannes Behl, Tobias Distler, and Rüdiger Kapitza. 2017. Hybrids on Steroids: SGX-Based High Performance BFT. In *Proceedings of the Twelfth European Conference on Computer Systems (EuroSys '17)*. ACM, 222–237.
- [8] Michael Ben-Or. Another Advantage of Free Choice: Completely Asynchronous Agreement Protocols (Extended Abstract). In *Proceedings of the Second Annual ACM Symposium on Principles of Distributed Computing (PODC '83)*.
- [9] Alysson Neves Bessani, João Sousa, and Eduardo Adílio Pelinson Alchieri. 2014. State Machine Replication for the Masses with BFT-SMART. In *44th Annual IEEE/IFIP International Conference on Dependable Systems and Networks (DSN'14)*. IEEE, 355–362.
- [10] Richard E Blahut. 1983. *Theory and Practice of Error Control Codes*. Vol. 126. Addison-Wesley.
- [11] Alexandra Boldyreva. 2003. Threshold Signatures, Multisignatures and Blind Signatures Based on the Gap-Diffie-Hellman-Group Signature Scheme. In *Public Key Cryptography — PKC 2003*. Springer, 31–46.
- [12] Dan Boneh, Ben Lynn, and Hovav Shacham. 2001. Short Signatures from the Weil Pairing. In *Advances in Cryptology — ASIACRYPT 2001*. Springer, 514–532.
- [13] Ethan Buchman. 2016. *Tendermint: Byzantine Fault Tolerance in the Age of Blockchains*. Ph.D. Dissertation.
- [14] Ethan Buchman, Jae Kwon, and Zarko Milosevic. 2018. The Latest Gossip on BFT Consensus. *CoRR* abs/1807.04938 (2018). <http://arxiv.org/abs/1807.04938>
- [15] Vitalik Buterin and Virgil Griffith. 2017. Casper the Friendly Finality Gadget. *CoRR* abs/1710.09437 (2017). <http://arxiv.org/abs/1710.09437>
- [16] Neal Cardwell, Yuchung Cheng, C. Stephen Gunn, Soheil Hassas Yeganeh, and Van Jacobson. 2016. BBR: Congestion-Based Congestion Control: Measuring Bottleneck Bandwidth and Round-Trip Propagation Time. *Queue* 14, 5 (2016), 20–53.
- [17] Miguel Castro and Barbara Liskov. 1999. Practical Byzantine Fault Tolerance. In *Proceedings of the Third Symposium on Operating Systems Design and Implementation (OSDI '99)*. USENIX Association, 173–186.
- [18] Benjamin Y Chan and Elaine Shi. 2020. Streamlet: Textbook Streamlined Blockchains. *Cryptography ePrint Archive*, Report 2020/088. (2020). <https://eprint.iacr.org/2020/088>.
- [19] T-H. Hubert Chan, Rafael Pass, and Elaine Shi. 2018. PaLa: A Simple Partially Synchronous Blockchain. *Cryptography ePrint Archive*, Report 2018/981. (2018). <https://eprint.iacr.org/2018/981>.
- [20] Byung-Gon Chun, Petros Maniatis, Scott Shenker, and John Kubiatowicz. 2007. Attested Append-Only Memory: Making Adversaries Stick to Their Word. In *Proceedings of Twenty-First ACM SIGOPS Symposium on Operating Systems Principles (SOSP '07)*. ACM, 189–204.
- [21] Tyler Crain, Christopher Natoli, and Vincent Gramoli. 2021. Red Belly: A Secure, Fair and Scalable Open Blockchain. (2021).
- [22] Ivan Damgård and Maciej Koprowski. 2001. Practical Threshold RSA Signatures without a Trusted Dealer. In *Advances in Cryptology — EUROCRYPT 2001*. Springer, 152–165.
- [23] Sisi Duan, Michael K. Reiter, and Haibin Zhang. 2018. BEAT: Asynchronous BFT Made Practical. In *Proceedings of the 2018 ACM SIGSAC Conference on Computer and Communications Security (CCS '18)*. ACM, 2028–2041.
- [24] Cynthia Dwork, Nancy Lynch, and Larry Stockmeyer. 1988. Consensus in the Presence of Partial Synchrony. *J. ACM* 35, 2 (1988), 288–323.
- [25] Parinya Ekparinya, Vincent Gramoli, and Guillaume Jourjon. 2020. The Attack of the Clones Against Proof-of-Authority. In *27th Annual Network and Distributed System Security Symposium (NDSS '20)*. The Internet Society.
- [26] Ethereum. 2013. Ethereum is a global, open-source platform for decentralized applications. <https://ethereum.org>. (2013).

- [27] Ittay Eyal, Adem Efe Gencer, Emin Gün Sirer, and Robbert van Renesse. 2016. Bitcoin-NG: A Scalable Blockchain Protocol. In *13th USENIX Symposium on Networked Systems Design and Implementation (NSDI '16)*. USENIX Association, 45–59.
- [28] Ittay Eyal and Emin Gün Sirer. 2014. Majority Is Not Enough: Bitcoin Mining Is Vulnerable. In *Financial Cryptography and Data Security*. Springer, 436–454.
- [29] Michael J. Fischer, Nancy A. Lynch, and Mike Paterson. 1983. Impossibility of Distributed Consensus with One Faulty Process. In *Proceedings of the Second ACM SIGACT-SIGMOD Symposium on Principles of Database Systems (PODS '83)*. ACM, 1–7.
- [30] Yossi Gilad, Rotem Hemo, Silvio Micali, Georgios Vlachos, and Nickolai Zeldovich. 2017. Algorand: Scaling Byzantine Agreements for Cryptocurrencies. In *Proceedings of the 26th Symposium on Operating Systems Principles (SOSP '17)*. ACM, 51–68.
- [31] Guy Golan-Gueta, Ittai Abraham, Shelly Grossman, Dahlia Malkhi, Benny Pinkas, Michael K. Reiter, Dragos-Adrian Seredinschi, Orr Tamir, and Alin Tomescu. 2019. SBFT: A Scalable and Decentralized Trust Infrastructure. In *49th Annual IEEE/IFIP International Conference on Dependable Systems and Networks (DSN'19)*. IEEE, 568–580.
- [32] Rachid Guerraoui. 2008. The Next 700 BFT Protocols. In *Principles of Distributed Systems*. Springer, 1–1.
- [33] Bingyong Guo, Zhenliang Lu, Qiang Tang, Jing Xu, and Zhenfeng Zhang. 2020. Dumbo: Faster Asynchronous BFT Protocols. In *Proceedings of the 2020 ACM SIGSAC Conference on Computer and Communications Security (CCS '20)*. Association for Computing Machinery, 803–818.
- [34] Ethan Heilman, Alison Kendler, Aviv Zohar, and Sharon Goldberg. 2015. Eclipse Attacks on Bitcoin's Peer-to-Peer Network. In *24th USENIX Security Symposium (USENIX Security 15)*. USENIX Association, 129–144.
- [35] IBM. 2021. AIX 7.1 - Software models. <https://www.ibm.com/docs/en/aix/7.1?topic=processes-software-models>. (2021).
- [36] Flavio Paiva Junqueira, Benjamin C. Reed, and Marco Serafini. 2011. Zab: High-Performance Broadcast for Primary-Backup Systems. In *Proceedings of the 2011 IEEE/IFIP International Conference on Dependable Systems and Networks (DSN'11)*. IEEE, 245–256.
- [37] Ghassan O. Karame, Elli Androulaki, and Srdjan Capkun. 2012. Double-Spending Fast Payments in Bitcoin. In *Proceedings of the 2012 ACM Conference on Computer and Communications Security (CCS '12)*. ACM, 906–917.
- [38] Aggelos Kiayias and Alexander Russell. 2018. Ouroboros-BFT: A Simple Byzantine Fault Tolerant Consensus Protocol. *Cryptology ePrint Archive*, Report 2018/1049. (2018). <https://eprint.iacr.org/2018/1049>.
- [39] Aggelos Kiayias, Alexander Russell, Bernardo David, and Roman Oliynykov. 2017. Ouroboros: A Provably Secure Proof-of-Stake Blockchain Protocol. In *Advances in Cryptology – CRYPTO 2017*. Springer, 357–388.
- [40] E. Kokoris-Kogias, P. Jovanovic, L. Gasser, N. Gailly, E. Syta, and B. Ford. 2018. OmniLedger: A Secure, Scale-Out, Decentralized Ledger via Sharding. In *2018 IEEE Symposium on Security and Privacy (SP)*. 583–598.
- [41] Ramakrishna Kotla, Lorenzo Alvisi, Michael Dahlin, Allen Clement, and Edmund L. Wong. 2007. Zzyzzyva: Speculative Byzantine Fault Tolerance. In *Proceedings of Twenty-First ACM SIGOPS Symposium on Operating Systems Principles (SOSP '07)*. ACM, 45–58.
- [42] Yujin Kwon, Dohyun Kim, Yunmok Son, Eugene Vasserman, and Yongdae Kim. 2017. Be Selfish and Avoid Dilemmas: Fork After Withholding (FAW) Attacks on Bitcoin. In *Proceedings of the 2017 ACM SIGSAC Conference on Computer and Communications Security (CCS '17)*. ACM, 195–209.
- [43] Leslie Lamport, Robert E. Shostak, and Marshall C. Pease. 1982. The Byzantine Generals Problem. *ACM Trans. Program. Lang. Syst.* 4, 3 (1982), 382–401.
- [44] Dave Levin, John R. Douceur, Jacob R. Lorch, and Thomas Moscibroda. 2009. TrInc: Small Trusted Hardware for Large Distributed Systems. In *Proceedings of the 6th USENIX Symposium on Networked Systems Design and Implementation (NSDI'09)*. USENIX Association, 1–14.
- [45] Fabio Ludovici and Hagen Paul Pfeifer. 2011. NetEm - Network Emulator. <https://www.linux.org/docs/man8/tc-netem.html>. (2011).
- [46] Loi Luu, Viswesh Narayanan, Chaodong Zheng, Kunal Baweja, Seth Gilbert, and Prateek Saxena. 2016. A Secure Sharding Protocol For Open Blockchains. In *Proceedings of the 2016 ACM SIGSAC Conference on Computer and Communications Security (CCS '16)*. ACM, 17–30.
- [47] Jean-Philippe Martin and Lorenzo Alvisi. 2005. Fast Byzantine Consensus. In *2005 International Conference on Dependable Systems and Networks (DSN'05)*. IEEE, 402–411.
- [48] Andrew Miller, Yu Xia, Kyle Croman, Elaine Shi, and Dawn Song. 2016. The Honey Badger of BFT Protocols. In *Proceedings of the 2016 ACM SIGSAC Conference on Computer and Communications Security (CCS '16)*. ACM, 31–42.
- [49] Satoshi Nakamoto. 2008. Bitcoin: A Peer-to-Peer Electronic Cash System. <https://bitcoin.org/bitcoin.pdf>. (2008).
- [50] C. Natoli and V. Gramoli. 2017. The Balance Attack or Why Forkable Blockchains are Ill-Suited for Consortium. In *2017 47th Annual IEEE/IFIP International Conference on Dependable Systems and Networks (DSN'17)*. IEEE, 579–590.
- [51] Jianyu Niu, Fangyu Gai, Mohammad Jalalzai, and Chen Feng. 2021. On the Performance of Pipelined HotStuff. In *IEEE INFOCOM 2021 - IEEE Conference on Computer Communications*. IEEE.
- [52] Rafael Pass and Elaine Shi. 2017. Hybrid Consensus: Efficient Consensus in the Permissionless Model. In *31st International Symposium on Distributed Computing, DISC 2017 (LIPIcs)*, Vol. 91. Schloss Dagstuhl - Leibniz-Zentrum für Informatik, 39:1–39:16.
- [53] Rafael Pass and Elaine Shi. 2018. Thunderella: Blockchains with Optimistic Instant Confirmation. In *Advances in Cryptology – EUROCRYPT 2018*. Springer, 3–33.
- [54] Marshall C. Pease, Robert E. Shostak, and Leslie Lamport. 1980. Reaching Agreement in the Presence of Faults. *J. ACM* 27, 2 (1980), 228–234.
- [55] I. S. Reed and G. Solomon. 1960. Polynomial Codes Over Certain Finite Fields. *Journal of The Society for Industrial and Applied Mathematics* 8, 2 (1960), 300–304. <https://academic.microsoft.com/paper/2148575324>
- [56] Fred B. Schneider. 1990. Implementing Fault-Tolerant Services Using the State Machine Approach: A Tutorial. *ACM Comput. Surv.* 22, 4 (1990), 299–319.
- [57] David Schwartz, Noah Youngs, Arthur Britto, et al. 2014. The Ripple Protocol Consensus Algorithm. *Ripple Labs Inc White Paper* 5, 8 (2014), 151.
- [58] Elaine Shi. 2019. Streamlined Blockchains: A Simple and Elegant Approach (A Tutorial and Survey). In *Advances in Cryptology – ASIACRYPT 2019*. Springer, 3–17.
- [59] Victor Shoup. 2000. Practical Threshold Signatures. In *Advances in Cryptology – EUROCRYPT 2000*. Springer, 207–220.
- [60] Gauthier Voron and Vincent Gramoli. 2019. Dispel: Byzantine SMR with Distributed Pipelining. *CoRR* abs/1912.10367 (2019). <http://arxiv.org/abs/1912.10367>
- [61] Wikipedia. 2020. Two-tree Broadcast. https://en.wikipedia.org/wiki/Two-tree_broadcast. (2020).
- [62] Wikipedia. 2021. The DAO. [https://en.wikipedia.org/wiki/The_DAO_\(organization\)](https://en.wikipedia.org/wiki/The_DAO_(organization)). (2021).
- [63] Wikipedia. 2021. HTTP persistent connection. https://en.wikipedia.org/wiki/HTTP_persistent_connection. (2021).
- [64] Maofan Yin, Dahlia Malkhi, Michael K. Reiter, Guy Golan-Gueta, and Ittai Abraham. 2019. HotStuff: BFT Consensus with Linearity and Responsiveness. In *Proceedings of the 2019 ACM Symposium on Principles of Distributed Computing (PODC '19)*. ACM, 347–356.
- [65] Maofan Yin, Dahlia Malkhi, Michael K. Reiter, Guy Golan Gueta, and Ittai Abraham. 2019. HotStuff: BFT Consensus in the Lens of Blockchain. (2019). <https://arxiv.org/abs/1803.05069v6>
- [66] Ted Yin. 2019. libhotstuff. <https://github.com/hot-stuff/libhotstuff>. (2019).
- [67] Mahdi Zamani, Mahnush Movahedi, and Mariana Raykova. 2018. RapidChain: Scaling Blockchain via Full Sharding. In *Proceedings of the 2018 ACM SIGSAC Conference on Computer and Communications Security (CCS '18)*. ACM, 931–948.